



## Dynamical and collisional evolution of Kuiper Belt binaries

Journal:	<i>Monthly Notices of the Royal Astronomical Society</i>
Manuscript ID:	MN-15-2500-MJ
Manuscript type:	Main Journal
Date Submitted by the Author:	06-Aug-2015
Complete List of Authors:	Brunini, Adrian; CONICET, Zanardi, Macarena
Keywords:	Kuiper belt: general < Planetary Systems

SCHOLARONE™  
Manuscripts

1  
2  
3  
4  
5  
6  
7  
8 **Dynamical and collisional evolution of Kuiper**  
9 **Belt binaries**  
10

11  
12  
13  
14  
15 Adrián Brunini<sup>1</sup> and Macarena Zanardi<sup>1,2</sup>  
16

17  
18  
19 *1: Grupo de Ciencias Planetarias, Facultad de Ciencias Astronómicas y*  
20 *Geofísicas. UNLP*

21 *2: IALP - CCT La Plata, CONICET*  
22 *Paseo del Bosque s/n (1900) La Plata, Argentina*  
23 *E-mail: abrunini@yahoo.com.ar*  
24  
25  
26  
27  
28  
29  
30  
31  
32  
33  
34  
35  
36  
37  
38  
39  
40  
41  
42  
43  
44  
45  
46  
47  
48  
49  
50

51 Number of pages: 25

52 Number of Figures: 11

53 Number of Tables: 1  
54  
55  
56  
57  
58  
59  
60

1  
2  
3  
4  
5  
6  
7  
8 Proposed running head: **Evolution of Binary TNOs**  
9  
10  
11  
12  
13  
14  
15  
16

17 Correspondence should be directed to:  
18  
19

20  
21 Adrián Brunini  
22 Facultad de Ciencias Astronómicas y Geofísicas  
23 Paseo del Bosque s/n  
24 La Plata (1900) Argentina  
25 E-mail: [abrunini@yahoo.com.ar](mailto:abrunini@yahoo.com.ar)  
26  
27  
28  
29  
30  
31  
32  
33  
34  
35  
36  
37  
38  
39  
40  
41  
42  
43  
44  
45  
46  
47  
48  
49  
50  
51  
52  
53  
54  
55  
56  
57  
58  
59  
60

### Abstract

We present numerical simulations of the evolution of synthetic Trans Neptunian Binaries (TNBs) under the influence of solar perturbations, tidal friction, and collisions with the population of Classical Kuiper Belt Object (KBOs).

We show that these effects, acting together, have strongly sculpted the primordial population of TNBs. If the population of Classical KBOs have a power law size distribution as the ones that are inferred from the most recent deep ecliptic surveys (Adams et al. 2014, Fraser et al. 2014), the fraction of surviving binaries at present would be of only  $\sim 70\%$  of the primordial population. The orbits of the surviving systems match reasonably well the observed sample.

Because of the impulse imparted during the collisional process, only  $\sim 10\%$  of the objects reach total orbital circularization ( $e \leq 10^{-4}$ ), and very few contact binaries should exist in the Trans Neptunian region.

Ultra wide binaries are naturally obtained in number and orbital distribution similar to the ones of the observed population, as a natural result of the combined action of KCTF and collisional evolution on an initial population of tight binaries.

KEYWORDS: Kuiper belt - Binaries

# 1 INTRODUCTION

The observational evidence suggests that binary objects in the trans neptunian region (hereafter TNBs) represent more than 11 % of the whole sample of observed objects in this region (Stephens & Noll 2006, Noll et al. 2008a, Grundy et al. 2009, 2011, Parker et al. 2011).

The observed magnitude of the components of the TNBs discovered so far suggests that most of them are systems formed by companions of nearly equal size.

The separation of the observed TNBs with determined orbital parameters (taken from the list at <http://www.johnstonsarchive.net/astro/astmoons>) vs. the size ratio is shown in Fig. (1), where we have limited the sample to systems with  $D_{PRIM} < 250$  km.

Most known TNBs are tight systems, where both components are separated less than 10 % of their mutual Hill Radius, defined as:

$$R_H = a_{\odot}(1 - e_{\odot}) \left( \frac{M_{bin}}{3M_{\odot}} \right)^{1/3}, \quad (1)$$

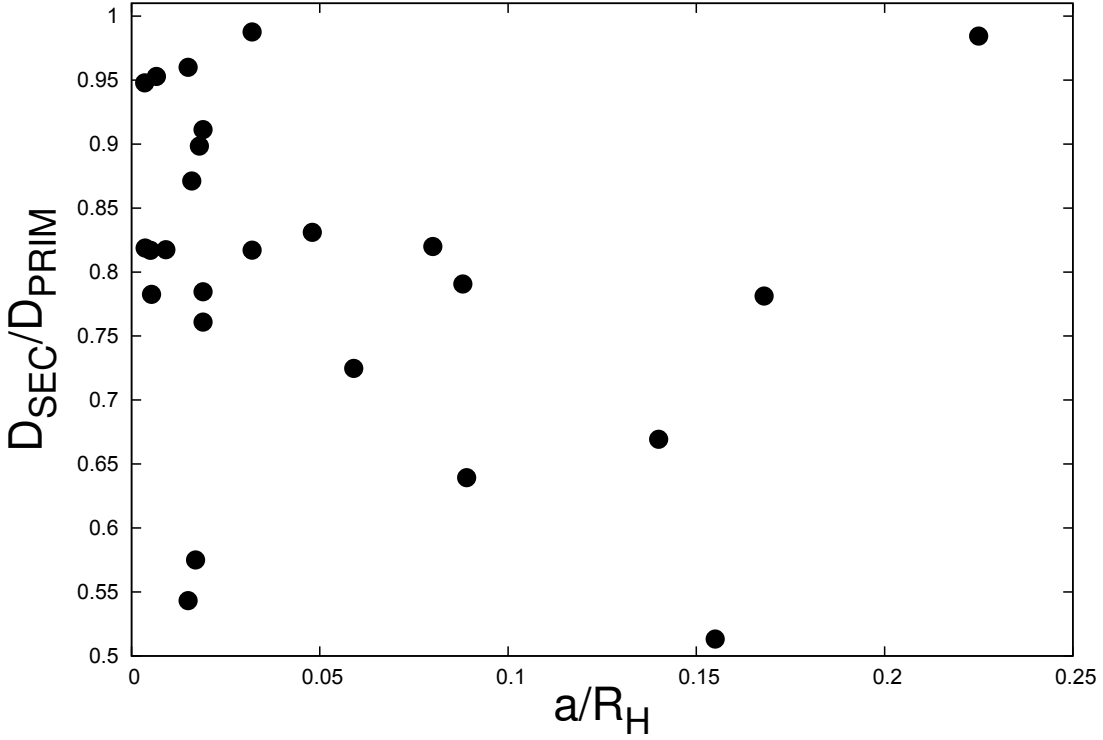
where  $a_{\odot}$  and  $e_{\odot}$  are the semi major axis and eccentricity of the binary heliocentric orbit respectively,  $M_{bin} = M_{prim} + M_{sec}$  is the combined mass of the primary and secondary components, and  $M_{\odot}$  is the solar mass.

Several formation mechanisms have been proposed, but none of them can fully reproduce the properties of the observed population. Nevertheless, the final product of any formation mechanism should reproduce the primordial distributions of physical and orbital parameters of the TNB population rather than the present ones. The present characteristics of the population of TNBs could be different than the primordial ones, as post formation orbital evolution could erase some primordial features. In fact, Porter & Grundy (2012) have recently performed numerical simulations of the post formation dynamical evolution of TNBs, subject to mutual tidal friction and solar perturbations, the so called KCTF evolution. These effects, acting on the age of the solar system, have strongly sculpted the orbital properties of TNBs. But Kozai cycles and tidal friction are not the only mechanisms that were acting along the age of the solar system.

Nesvorný et al. (2011) performed numerical simulations of the collisional grinding of wide TNBs. The exchange of impulse at impact on one of the components can change the binary orbit. In this paper, the effect of successive collisions was treated as a random walk dynamical diffusion of the orbital elements. Nesvorný et al. (2011) found that wide binaries are easily disrupted, and that during a period of intense collisional evolution, a trend of decreasing binary fraction with decreasing radius would be imprinted on

1  
2  
3  
4  
5  
6  
7  
8  
9  
10  
11  
12  
13  
14  
15  
16  
17  
18  
19  
20  
21  
22  
23  
24  
25  
26  
27  
28  
29  
30  
31  
32  
33  
34  
35  
36  
37  
38  
39  
40  
41  
42  
43  
44  
45  
46  
47  
48  
49  
50  
51  
52  
53  
54  
55  
56  
57  
58  
59  
60

Figure 1: *Size ratios of the known trans neptunian binaries with  $D \leq 250$  km.*



the present TNB population. In addition, the relative excess of tight binaries with respect to wide ones, was attributed to the fact that wide TNBs, despite easier to detect, are fragile with respect to external perturbers, such as close encounters with Neptune (Parker & Kavelaars 2010) or collisions with the population of TNOs (Petit & Mousis 2004; Nesvorný et al. 2011). Parker & Kavelaars (2012) performed numerical simulations of the collisional evolution of ultra wide TNBs ( $a > 0.07R_H$ ). They have found that it is unlikely for the ultra-wide binaries to have evolved from an initially tighter population, because collisions cannot produce a widened population with an inclination distribution as cold as is observed for the ultra-wide binaries.

Up to the present, there are not simulations of the orbital evolution of a primordial population of TNBs including KCTF and collisions. In the simulations of Porter & Grundy (2012), collisional effects were not included.

It is clear that the effects of collisions on the orbital properties of tight binaries cannot be treated as a random walk process, because changes in the binary orbit produced by the exchange of impulse during collisions, could be attenuated, and even erased by tidal evolution.

In order to advance in our knowledge of the primordial characteristics of the population of Trans Neptunian Binaries, we present here a series of numerical simulations including orbital, rotational and physical evolution produced at collisions of TNBs with the population of Classical TNOs, including also KCTF orbital evolution.

In the next Section we describe our collisional and dynamical model, the initial conditions of our binary sample, and the population of impactors. We describe the results in Section 3 and the last Section is devoted to the conclusions.

## 2 THE MODEL

Our collisional model follows closely the simple model used by Parker & Kavelaars (2012) in their study of wide TNBs. In all the simulations, the radii of the objects were determined assuming a spherical shape and a given bulk density.

In this paper we consider that all collisions are produced at a relative velocity of  $V_i \sim 1 \text{ km s}^{-1}$ , the typical relative velocity for Kuiper Belt Objects.

Given a population of projectiles, the mean time between single impacts can be estimated as:

$$T_{col} = [P_i R_{bin}^2 N(R > R_{min})]^{-1}, \quad (2)$$

where  $P_i$  is the intrinsic collision probability. We adopt  $P_i = 1.3 \times 10^{-21} \text{ km}^{-2} \text{ yr}^{-2}$  for all our simulations (Farinella et al. 2000).  $R_{min}$  is the minimum impactor size radius and  $N(R > R_{min})$  is the total number of objects larger than  $R_{min}$ .  $R_{bin}$  is the radius of the target (one of the components of the TNB). For the population of projectiles, following Parker & Kavelaars (2012), we considered a minimum size of  $R_{min} = 100 \text{ m}$ . In eq. (2) the cross section of the projectile is neglected. Nevertheless, given a population of objects with a differential power law size distribution of the form:

$$\frac{dN}{dR} \propto R^{-q}. \quad (3)$$

The total number of collisions during a given interval of time is

$$N_{tot} = N(R_{bin}) \left( 1 + \frac{(q-1) R_{min}^2}{(q-3) R_{bin}^2} + 2 \frac{R_{min} (q-1)}{R_{bin} (q-2)} \right), \quad (4)$$

where  $N(R_{bin})$  is the number of collisions computed neglecting the cross section of the projectile. As  $R_{bin} \gg R_{min}$ , neglecting the radii of the projectile in the computation of the cross section does not introduce a significant error in  $T_{col}$ . Within this approximation, we have simulated the collisional evolution as follows: For each TNB, we have computed two independent sequences of collisions: One for the primary and another for the secondary component. For the primary component, we generate the total number of impacts  $N_{tot}^{PRIM}$  produced during the age of the solar system  $\tau = 4.5 \times 10^9 \text{ yr}$ , from a Poisson distribution with mean  $\tau/T_{col}^{PRIM}$ . We then sampled an array of times  $T_i^{PRIM}$ ,  $i = 1, N_{tot}^{PRIM}$  from uniform random deviates over the interval  $[0, \tau]$ . We also computed another series of  $N_{tot}^{SEC}$  times  $T_j^{SEC}$  for the secondary component. Both sequences are then combined and sorted forming an unique sequence of collision times. For each collision, a projectile is generated, whose radius is taken at random from a given size distribution function. As established by Petit & Mousis (2004) and later confirmed by Parker & Kavelaars (2012), only a small fraction of the binary mass (e.g. less than 10 %) is loss during non catastrophic collisions, and therefore the variation of the cross section by this effect would be

$$\frac{\Delta M}{M} = \frac{3}{2} \frac{\Delta R^2}{R^2}, \quad (5)$$

and this effect was not taken into account in our model.

We also considered mass loss during collisions by using the strength law for ice proposed by Benz & Asphaug (1999), which is valid for impacts at velocities of the order of  $0.5 - 3 \text{ km s}^{-1}$ . Based on the kinetic energy of the



projectile  $E_K$ , the mass  $M_R$  of the largest remaining fragment was estimated using the relationship

$$\gamma = \frac{M_R}{M_0} = 1 - 0.5 \frac{E_K}{M_0 Q_D}, \quad (6)$$

where  $M_0$  is the target mass and  $Q_D$  the specific energy required to disrupt 50 % of the mass of the parent body, which is given by

$$Q_D = 7 \times 10^7 \left( \frac{R_0}{1 \text{ cm}} \right)^{-0.45} + 2.1 \rho \left( \frac{R_0}{1 \text{ cm}} \right)^{1.19} \text{ erg g}^{-1}. \quad (7)$$

Collisions were produced at a random position on the target surface. The direction of the collisions were also generated at random, following Henon's recipe (Henon 1972). This allows us to compute the change of the components of the relative orbital velocity of the binary, and consequently of the orbital elements.

For collisions with  $\gamma > 0.8$ , momentum is almost conserved as if they were perfectly inelastic collisions. But if the mass loss is larger than 20 % a significant part of the projectile impulse goes with the ejected fragments, and linear and angular impulse is less effectively transferred to the remaining fragment. This effect was modeled following the recipe of Parker & Kavelaars (2012). They used a piece wise linear prescription to approximately reproduce the velocity of the largest remaining fragment found by Benz & Asphaug (1999), which is given by

$$V' = \min\{V'_0; (1.045 - 0.895\gamma)V_{esc}\}, \quad (8)$$

where  $V'_0$  is the velocity that would be expected if all of the momentum of the impactor is transferred to the largest remaining fragment, and  $V_{esc}$  is the escape velocity from the target.

Model the transfer of rotational angular momentum during non catastrophic collisions is a very complex task, not yet accomplished for icy targets. On basaltic targets, Yanagisawa & Hasegawa (2000) conducted high-velocity impact experiments to study the total angular impulse that a target acquires through a collisional process. Following this work, it is possible to write

$$\Delta L = \psi L_i, \quad (9)$$

where  $\Delta L$  is the angular momentum acquired by a spherical target during the collision,  $L_i$  denotes the pre-impact momentum of the projectile, and  $\psi$  is an efficiency factor. Yanagisawa & Hasegawa (2000) found that  $\psi$  is correlated with the incident angle of the projectile, measured from the normal to the target surface  $\theta$

$$\psi = \psi_0 \cos^2 \theta, \quad (10)$$

with  $\psi_0$  a constant depending on the target material, but rather independent of the impact relative velocity. For basaltic targets  $\psi_0 = 0.4$ . For sand targets Gault & Schultz (1986) found  $\psi_0 \sim 0.7$ . It is expected that  $\psi_0$  should be even large for ice, because the efficiency of angular momentum transfer increases with the projectile penetration (Yanagisawa 1994). Therefore, we adopted  $\psi_0 = 1$  in all our simulations.

After each impact, a new angular momentum vector is computed. To do this, we consider also the mass loss of the target after each impact. The mass loss  $\Delta M$  reduces the moment of inertia by an amount  $\Delta I$ . Assuming that the shape of the target remains spherical, we have

$$\frac{\Delta I}{I} = \frac{5}{3} \frac{\Delta M}{M}. \quad (11)$$

It is worth noting that the angular momentum transfer at collisions for the case of non spherical bodies is more efficient than for spherical ones. Nevertheless this is a second order effect that was not considered in our simulations.

Between successive collisions, binary orbits evolve according to the secular theory of Kozai cycles already used in Brunini (2014), which was based in Fabricky & Tremaine (2007). Our model also includes the evolution due to mutual tides, either on the binary orbit as on the diurnal rotation and obliquity of the binary components. For the tidal evolution model we have to adopt  $Q$ , the tidal dissipation function of the binary members, and  $K_L$  which is the second tidal Love number. We used the same definitions as in Porter & Grundy (2012) for them: for half of the cases, we adopted the canonical values for icy homogeneous solid bodies of  $Q = 100$ , density  $\rho = 1 \text{ g cm}^{-3}$  and

$$K_L = \frac{3}{2} \left( 1 + \frac{19\mu_r r}{2GM_{bin}\rho} \right), \quad (12)$$

with the rigidity  $\mu_r = 4 \times 10^9 \text{ N/m}^2$ . For the other half of the simulated cases we have assumed that the binary is composed by two icy rubble piles, with  $\rho = 0.5 \text{ g cm}^{-3}$  and

$$K_L = r/10^5 \text{ km}, \quad (13)$$

and  $Q = 10$ .

Following Porter & Grundy (2012), in all the simulations the components of the binary start separated at random between 2 and 10 % of their mutual

Hill radii. The inclination of the orbital planes were also taken at random between  $-90^\circ$  and  $90^\circ$  measured from the plane of the heliocentric orbit of the TNB. The eccentricity of the mutual orbit  $e_{bin}$ , was also taken at random between 0 and 0.9. The heliocentric orbit of the binary center of mass have  $a_\odot = 45$  AU and  $e_\odot = 0.05$  in all the simulated cases.

The binaries in the simulations have radii at random in the range  $30 \text{ km} \leq r \leq 100 \text{ km}$ . The primary was generated with a given cumulative size distribution also used to generate the population of projectiles. We explored the evolution of TNBs with  $D_{SEC}/D_{PRIM} = 1, 0.75, 0.5$  and we have also included runs with  $D_{SEC}/D_{PRIM} = 0.25$ . The motivation to do this was to analyze if the present size ratio of the observed sample, where predominantly both components are of the same size, is primordial or a result of a post formation evolution process.

There is at present a controversy about the size distribution of objects in the trans neptunian space. The most recent results are those reported by Adams et al. (2014) and Fraser et al. (2014). Both agree in the fact that the cumulative absolute magnitude distribution of objects is well represented by a double exponent power law of the form

$$N(\leq H) = \begin{cases} C 10^{\alpha_1 H} & H \leq H_b \\ C 10^{\alpha_1 H_b} 10^{\alpha_2 (H - H_b)} & H_b < H. \end{cases}$$

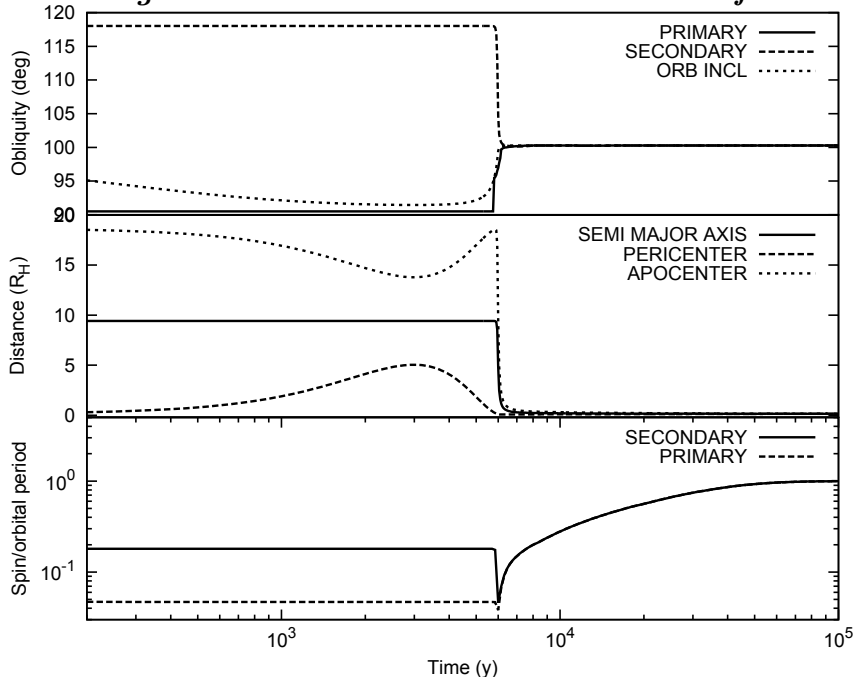
Fraser et al. (2014) considered the available surveys from which accurate absolute magnitude distribution of KBOs could be determined. Considering a mean albedo of  $p = 0.15$ , they found a break magnitude of  $H_b = 6.9$  (which corresponds to a break radius of  $r_b = 70 \text{ km}$ ) for the cold population of KBOs. They also found the slopes  $q_1 = 8.2$  and  $q_2 = 2.9$ .

On another hand, Adams et al. (2014) conducted a deep ecliptic survey yielding 304 objects with well determined orbits and dynamical classification. For the classical TNO population, they determined the parameters  $\alpha_1 = 1.02 \pm 0.01$ , and  $\alpha_2 = 0.42 \pm 0.02$ , in agreement with the observed population of Centaurs. They also obtained  $H_b = 7.2$ , corresponding to a breaking radius of  $R_b = 62 \text{ km}$ , if considering a mean albedo of 15 % (Fraser et al. 2014). As  $q = 5\alpha + 1$ , we found  $q_1 = 6.1$  and  $q_2 = 3.1$ . They also found that the total number of objects with  $H \leq 7$  in the Classical Kuiper Belt (Hot plus Cold populations) is  $N = 2100 \pm 300$  objects. We have adopted this size distribution function to carry out our numerical simulations.

It is worth noting that our collisional model is not self consistent, in the sense that we are neglecting the collisional and dynamical evolution of the population of projectiles in the Kuiper Belt.

The evolution of each TNB was followed for  $4.5 \times 10^9$  yr or stopped

Figure 2: *An example of KCFT evolution of an equal mass binary not including collisional evolution. See section 3 for details.*



if one of the following end states was reached: the system became unbound; impact itself; one of the components spun to breakup; the orbit circularizes reaching  $e < 10^{-4}$ ; both components reach the Roche distance ( $\sim 1.26(R_{PRIM} + R_{SEC})$ ) with low eccentricity (became a contact binary); one of the components is catastrophically disrupted by a collision.

In order to test our implementation of the KCFT secular model, we performed a series of simulations not including the collisional evolution. The results we found were consistent with those reported by Porter & Grundy (2012). As an example, in Fig. (2) we show the orbital and rotational evolution of a binary formed by two rubble-piles of equal mass, with  $Q = 10$  and radii of 42 km. The initial orbit have  $a = 0.097R_{Hill}$ ,  $e = 0.99$ , and inclination  $i = 99^\circ$ , the same values used by Porter & Grundy (2012) for the case they have shown in their Fig.(1).

Despite the orbital eccentricity being very high, the initial conditions are such that the Kozai mechanism is in the phase where the orbit becomes more circular and less inclined. The pericenter increases gradually, and therefore there is very little tidal evolution at the beginning of the simulation. After reaching a minimum of  $e = 0.46$  at  $t \sim 3000$  yr, the eccentricity starts to grow. As the pericentric distance shrinks, the tidal friction timescale becomes very short, and after  $\sim 6500$  yr of evolution the orbit becomes circular and

the separation of only  $0.015R_{Hill}$ . The spin axes end up aligned and the rotation rates equal the orbital motion. The agreement with the evolution shown in Porter & Grundy (2012) is remarkable good.

### 3 RESULTS

Figure 3: *Evolution of the semi major axis and eccentricity of three surviving binaries, were the interplay between collisions and tidal evolution is evident.*

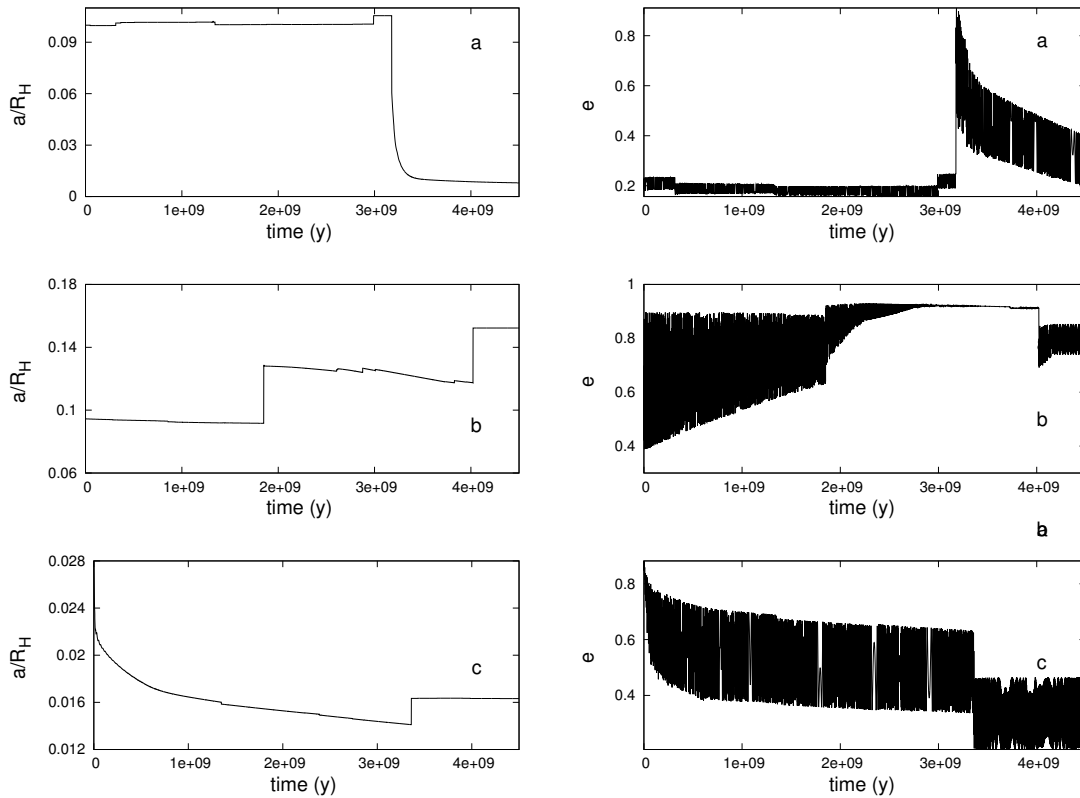


Fig. (3) shows three typical orbital evolution found in our simulations, where clearly the importance of including collisions and KCFT evolution acting together becomes evident. In panel *a* the binary starts with a separation of  $\sim 0.093R_H$ . As the orbital eccentricity is small, the pericentric distance is relatively large ( $\sim 0.06R_H$ ), and there is little tidal evolution. But at

1  
2  
3  
4  
5  
6  
7  
8  
9  $\sim 3.2 \times 10^9$  yr one of the components of the binary receives an impact. The  
10 exchange of impulse rises the eccentricity

11 up to 0.9 and the tidal friction time scale becomes very short. In the last  
12 Gy of evolution, the binary becomes tight, orbiting at only 1.5 % of the Hill  
13 radius. Panel *b* depicts the orbital evolution of a TNB that receives successive  
14 impulses, making the system more and more widely separated. In this case,  
15 KCTF does not play an important role, and a random-walk approximation  
16 including only collisional evolution, like to the model used by Nesvorný et al.  
17 (2011) and Parker & Kavelaars (2012), would be a good model. In Panel *c*,  
18 during the first  $t \sim 3 \times 10^9$  yr, the orbit of the TNB is gradually circularized  
19 by tidal friction. However, a collision onto one of the components increases  
20 the semi major axis, and decreases the eccentricity. In this new situation,  
21 tidal friction almost ceases to be operative, and the orbit stays at  $\sim 1.5$  %  
22 of  $R_{Hill}$  for the rest of the simulation.

23  
24  
25  
26 It results evident that any model of the primordial population of TNBs  
27 should include KCFT and collisional evolution acting together.  
28

### 29 30 3.1 Bulk statistics of the results

31  
32 Table 1 presents the bulk statistics of the results we have found in our simu-  
33 lations. We have adopted the orbital classification proposed by Parker et al.  
34 (2011):  
35

- 36 • Tight Binaries: TNBs with separation  $\leq 0.05R_{Hill}$ . In this category we  
37 have also included those binaries ending up with tight circular orbits  
38 (those circularized by tidal friction, reaching  $e \leq 10^{-4}$ ).
- 39 • Wide Binaries: those TNBs with intermediate separations ( $0.05R_{Hill} <$   
40  $a < 0.07R_{Hill}$ ).
- 41 • Ultra Wide Binaries: TNBs with  $a \geq 0.07R_{Hill}$ .

42  
43  
44  
45  
46 In total, 532 objects survive as TNBs  $4.5 \times 10^9$  yr. TNBs with very differ-  
47 ent size ratio ( $D_{SEC}/D_{PRIM} = 0.25$ ) are rather fragile systems. Only  $\sim 40$   
48 % survive the entire simulation. Nevertheless, the sample of observed TNBs  
49 with determined sizes for both components is  $N \sim 25$  ([www.johnstonsarchive.net](http://www.johnstonsarchive.net)).  
50 In our runs, the fraction of survivors with  $D_{SEC}/D_{PRIM} = 0.25$  is  $f =$   
51  $93/532 \sim 0.17$ , and therefore, there should be at least  $25 \times 0.17 \sim 4$  objects of  
52 this class in the population with known sizes. In Fig. (1) it is possible to ob-  
53 serve that there are not TNBs with  $D_{SEC}/D_{PRIM} \leq 0.5$ . Therefore, the first  
54 conclusion is that the primordial population of TNBs should be composed  
55 by systems whose components are of similar sizes, and then, in what follows,  
56  
57  
58  
59  
60

Table 1: *Statistics of the runs. SURVIVORS: objects surviving the entire simulation as TNBs. Tight: binaries with separations  $a/R_H \leq 0.05$ . CIRC: circularized orbits with  $e < 10^{-4}$  (they are also included in the Tight class). Wide: systems ending up with  $0.05 < a/R_H \leq 0.07$ . Ultra wide: systems with  $a/R_H > 0.07$ . CONT: objects reaching the Roche separation with almost circular orbit. DISRUPTED: systems not surviving the entire simulation. SEP: binaries with apocentric distance greater than the mutual Hill distance. COL: components colliding mutually. CAT: binaries in which one of the components receives a catastrophic collision.*

$D_{SEC}/D_{PRIM}$	Q	SURVIVORS					DISRUPTED		
		Tight	Circ	Wide	Ultra wide	Cont	Sep	Col	Cat
0.25	10	15	1	9	23	1	42	9	2
0.25	100	14	1	12	20	0	52	1	1
0.50	10	38	8	6	24	0	18	8	6
0.50	100	28	4	10	25	0	21	13	3
0.75	10	41	14	11	29	0	8	8	3
0.75	100	39	12	9	25	0	17	8	2
1.0	10	45	9	12	22	0	6	9	6
1.0	100	40	12	13	22	0	19	6	0

we will restrict our analysis to the simulations with  $D_{SEC}/D_{PRIM} \geq 0.5$ . In these three categories, the surviving fraction is  $439/600 \sim 0.73$

The results with  $D_{SEC}/D_{PRIM} = 1$  are directly comparable to those reported by Porter & Grundy (2012) for this case: They found that a large fraction (30 – 60 %) reaches circularization, and that only a small fraction (3 – 5 %) of the initial sample is disrupted. Our results are in contrast with these ones, showing that the collisional evolution plays a crucial role in the post formation evolution of the population of TNBs, being important not only for wide binaries, as it was already shown by Parker & Kavelaars (2012), but also for tight ones.

Almost in all the explored cases, the collisional evolution prevents the formation of contact binaries, defined as those reaching the Roche distance with a very small orbital eccentricity. The existence of three objects among the population of periodic comets (8P/Tuttle 67P/Churyumov-Gerasimenko and 103P/Hartley 2) being presumably contact binaries, might be interpreted as a result of their evolution as Binary Centaurs (Brunini, 2014), after they leave the Scattered Disk. In the frame of our model, the probability that they leave the Trans Neptunian region already as contact binaries is very small.

Only  $\sim 10$  % of the objects reach total circularization ( $e \leq 10^{-4}$ ). This fact can be explained by the impulse imparted in the collisional process. A projectile impacting on the secondary component of a binary, changes the orbital velocity  $v_{orb}$  by an amount  $\Delta v$ . Assuming an isotropic geometry for the collisions, a binary on circular orbit acquires, on average, an eccentricity that may be computed as (Danby, 1988)

$$\Delta e = \sqrt{\frac{5}{6}} \frac{\Delta v}{v_{orb}}. \quad (14)$$

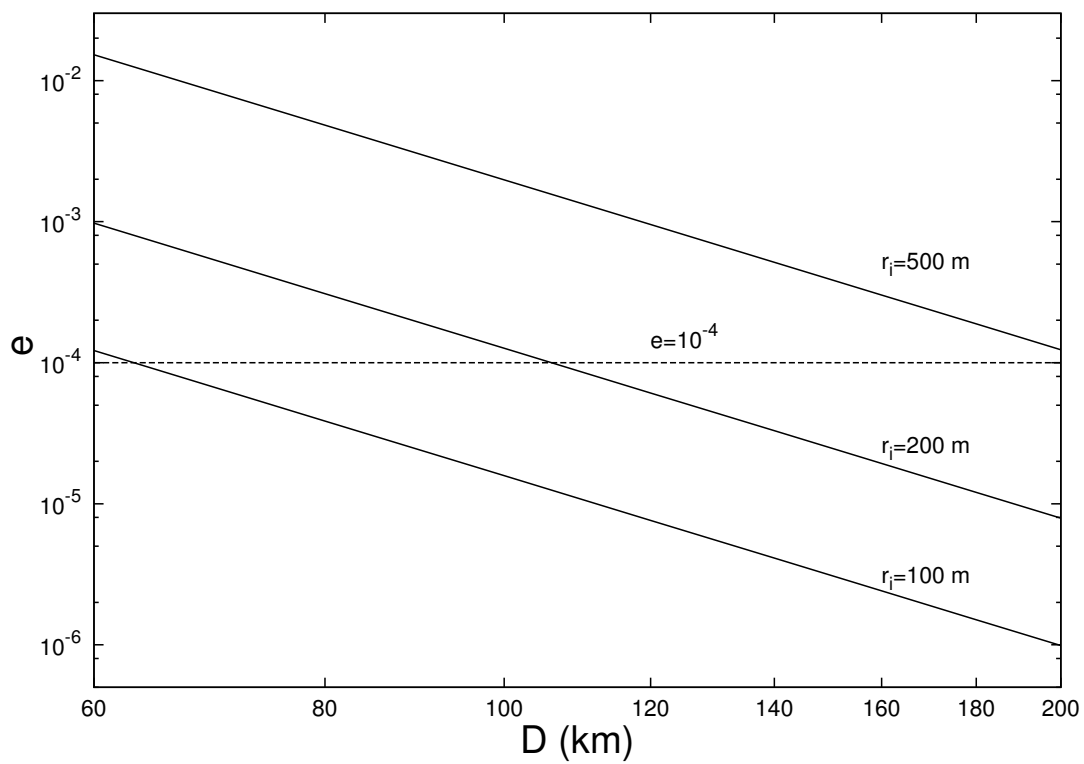
If the projectile have a mass  $m_i$ , and the impact is at a relative velocity  $v_i$ , we get

$$\Delta e \sim \sqrt{\frac{5}{6}} \frac{m_i}{M} \frac{v_i}{v_{orb}}, \quad (15)$$

where  $v_{orb}$  is the orbital velocity of the binary before the impact, and  $M$  is the target mass. Fig.(4) shows the eccentricity acquired by a binary with components of equal size, orbiting on a circular orbit at 1 %  $R_{Hill}$ , for three different impactor sizes. It may be observed that a collision of a projectile of  $r_i \geq 100$  m could excite an eccentricity larger than our criterion for circularization, explaining why these end states are so rare in our simulations.



Figure 4: *Orbital eccentricity that a tight binary on circular orbit acquires in a single collision.*



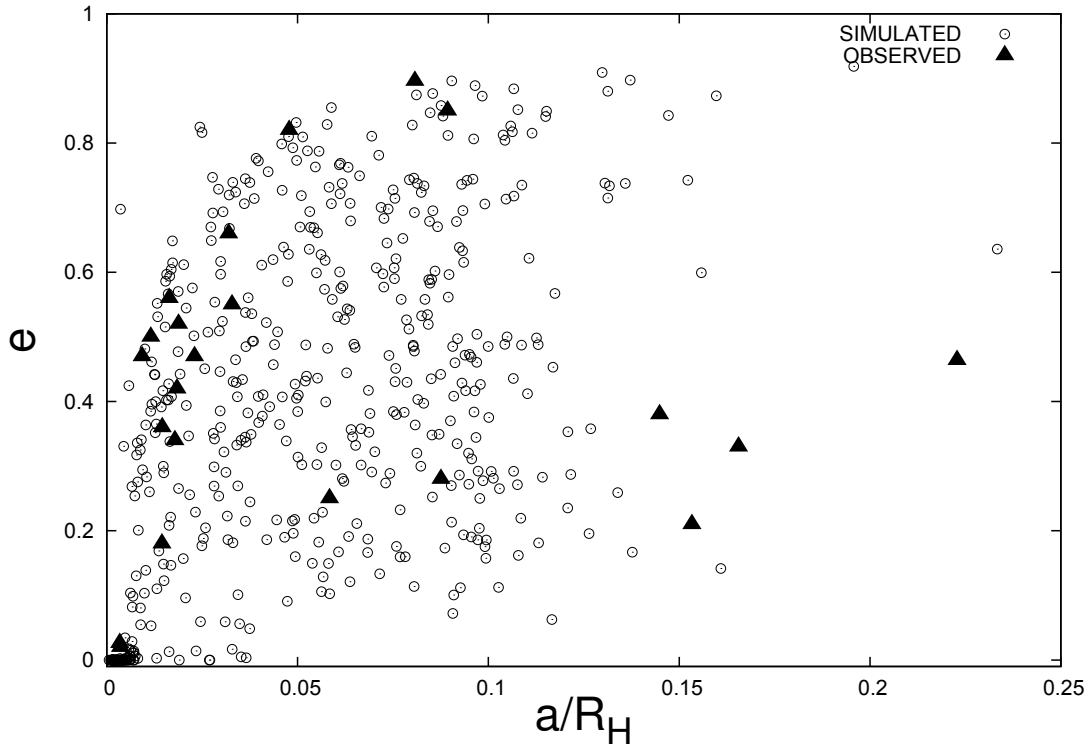


Figure 5: *Semi major axis vs. eccentricity of the surviving binaries.*

Roughly 7 % of the binaries separate as couples of single objects. Less than 4 % of the initial binaries received a catastrophic collision, mainly because the number of collisions is relatively small and the impactors are in the tail of small objects of the size distribution function. As expected, rubble piles are more prone to be catastrophically disrupted.

### 3.2 Orbital and rotational properties of the surviving TNBs

Fig.(5) and Fig. (6) show the final distribution of orbital eccentricities and inclinations of the surviving systems.

As expected, there is an accumulation of binaries with circular orbits at small separations. The mutual inclinations depart from an uniform distribution. As it is known (Porter & Grundy 2012) KCTF preserves the prograde / retrograde ratio of the initial distribution, and as collisions in our model

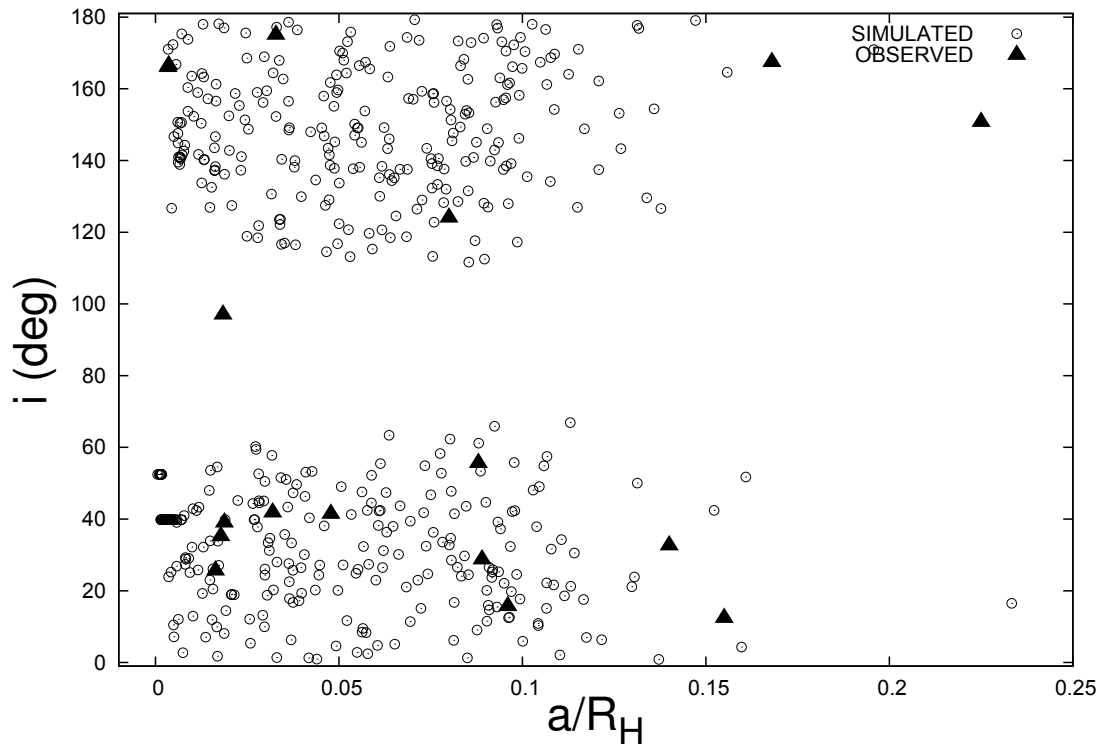


Figure 6: *Semi major axis vs. orbital inclination of the surviving binaries. Few observed binaries have  $i$  determined.*

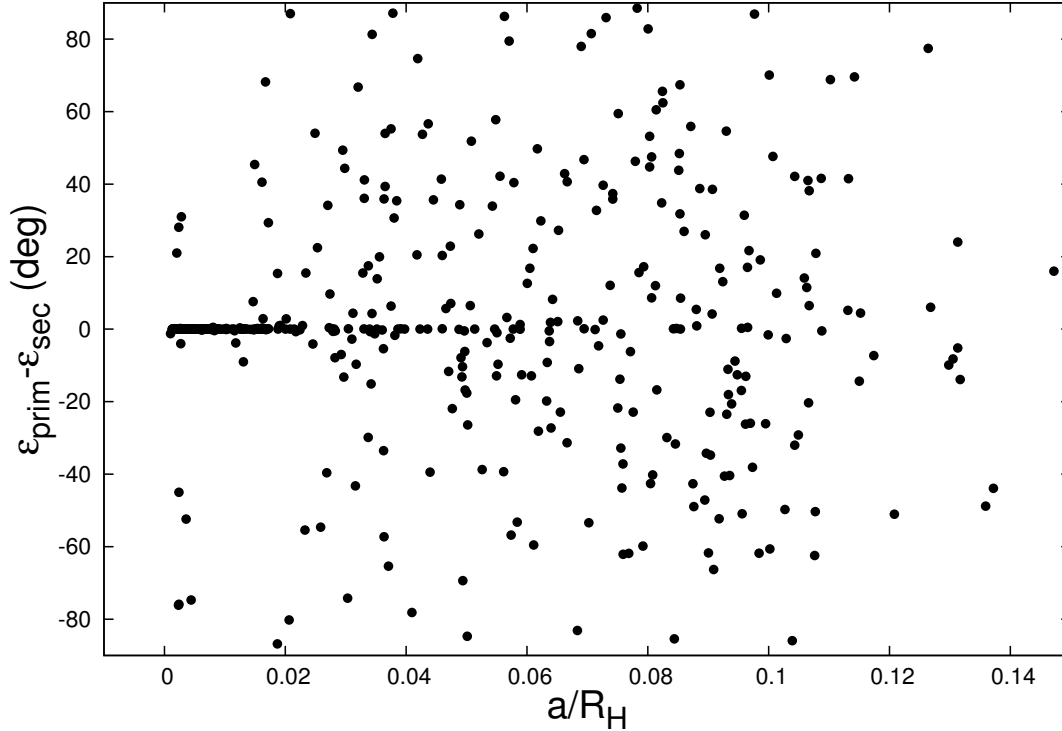


Figure 7: *Difference between the orientations of the spin axes of both components. Tight binaries end up with their spin axes aligned.*

are oriented at random, this feature is also observed in the distribution of orbital inclinations shown in Fig. (6).

Regarding the evolution of the obliquity and the spin period of the binaries, we found results very similar to the ones reported by Porter & Grundy (2012). The obliquity and spin period end states are shown in Fig. (7) and Fig. (8).

The obliquity of very tight binaries evolve to end states with aligned spin axes, a feature not observed in wide systems because of their weaker tidal interaction. In addition, as it is shown in Fig. (8), the diurnal rotation rate of very tight TNBs tends to be synchronized with the orbital mean motion. Few cases depart from this behavior, but all of them are systems reaching circularization ( $e < 10^{-4}$ ). In all these cases the simulations did not complete the 4.5 Gy of evolution, and a collision changes the rotational angular momentum of one of the components. As the orbits are strongly

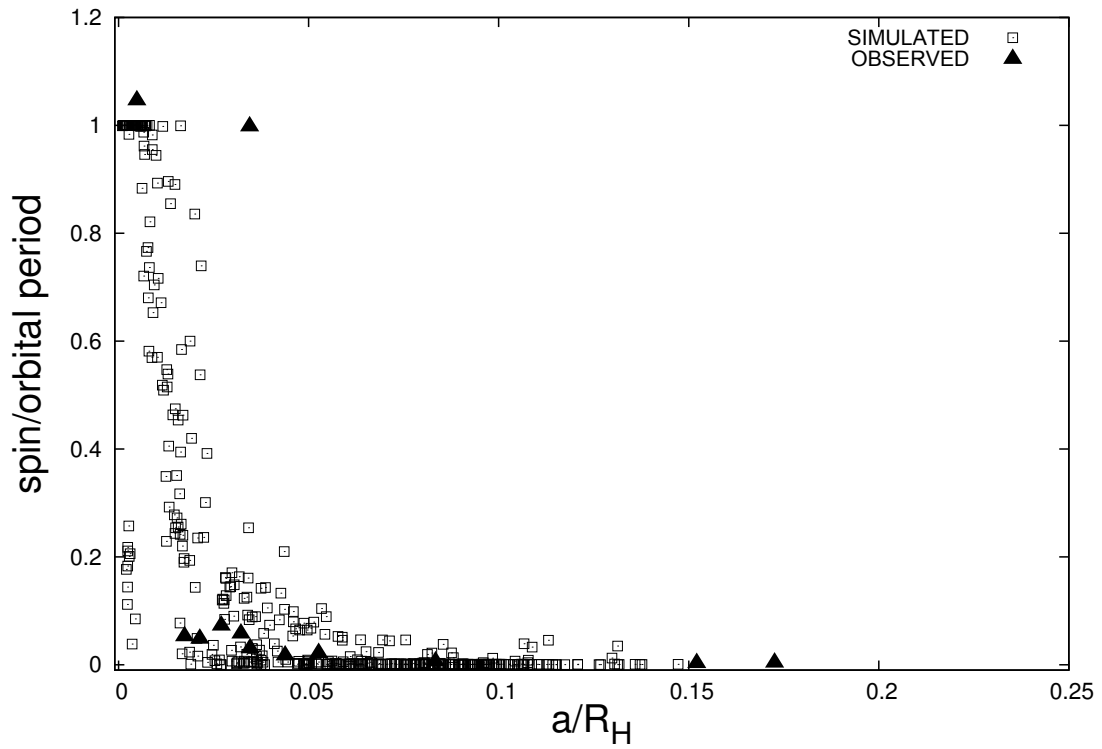
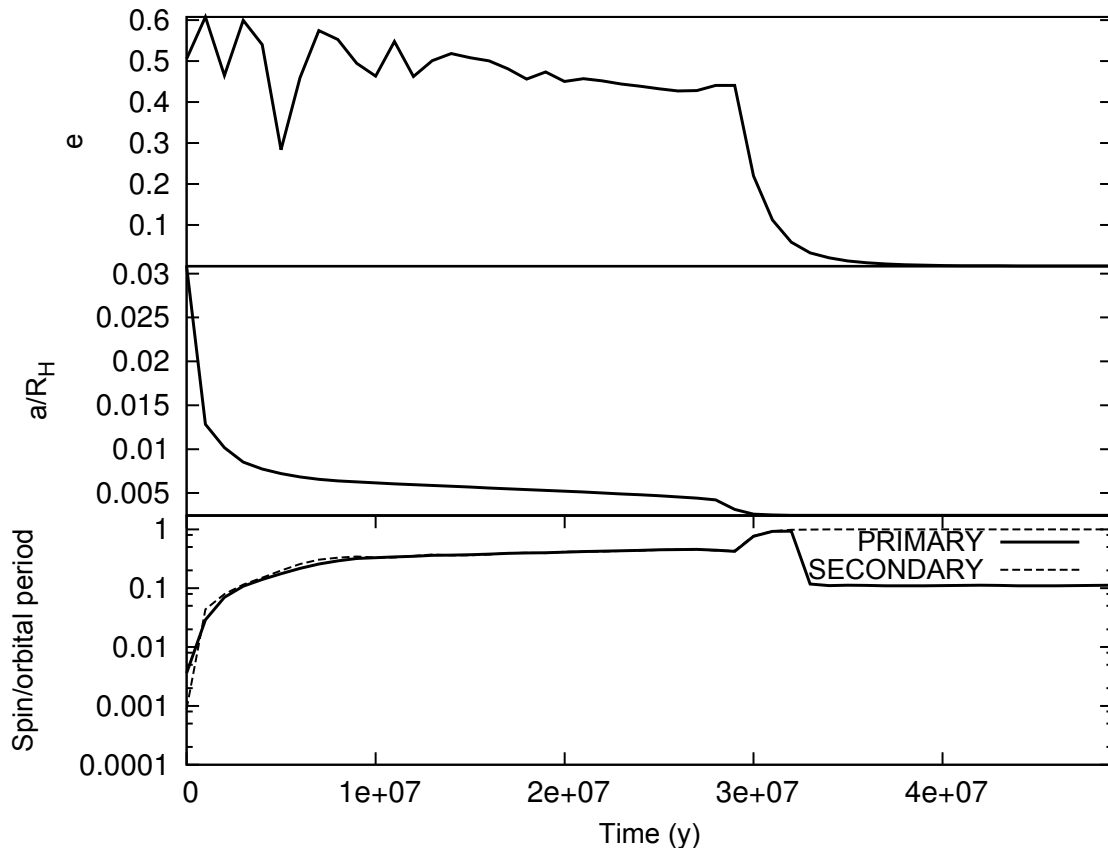


Figure 8: *The spin period of the surviving objects in the simulations.*

1  
2  
3  
4  
5  
6  
7  
8  
9  
10  
11  
12  
13  
14  
15  
16  
17  
18  
19  
20  
21  
22  
23  
24  
25  
26  
27  
28  
29  
30  
31  
32  
33  
34  
35  
36  
37  
38  
39  
40  
41  
42  
43  
44  
45  
46  
47  
48  
49  
50  
51  
52  
53  
54  
55  
56  
57  
58  
59  
60

Figure 9: *Orbital and rotational evolution of a circularized system suffering a collision at  $\sim 3 \times 10^7$  y. The collision onto the primary component decouples the spin period of both objects.*



bounded, the impacts could not change substantially the eccentricities and the semi major axes. One of these behaviors is shown in Fig (9).

### 3.3 Ultra wide binaries

Tight to moderately wide binaries represent 30 % of the cold classical population of TNOs (Noll et al. 2008), whereas the fraction of ultra wide binaries is estimated to be  $\sim 5$  % of the current binary population (Lin et al. 2010). In Table 1 it is shown that  $\sim 35$  % of the surviving systems are ultra wide binaries. Most of them are systems whose initial separations were  $\geq 0.07R_H$ . However, 20 initially tight binaries, starting with  $a < 0.05R_{Hill}$ , end up as ultra wide binaries, with  $a > 0.07R_{Hill}$ . This objects represent 4.4 % of the final sample of surviving binaries, a number which is in agreement with the fraction of known ultra wide binaries.

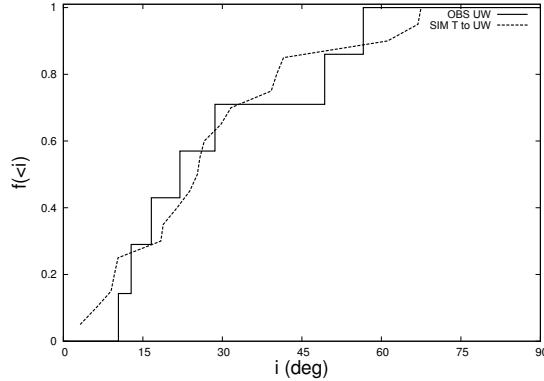
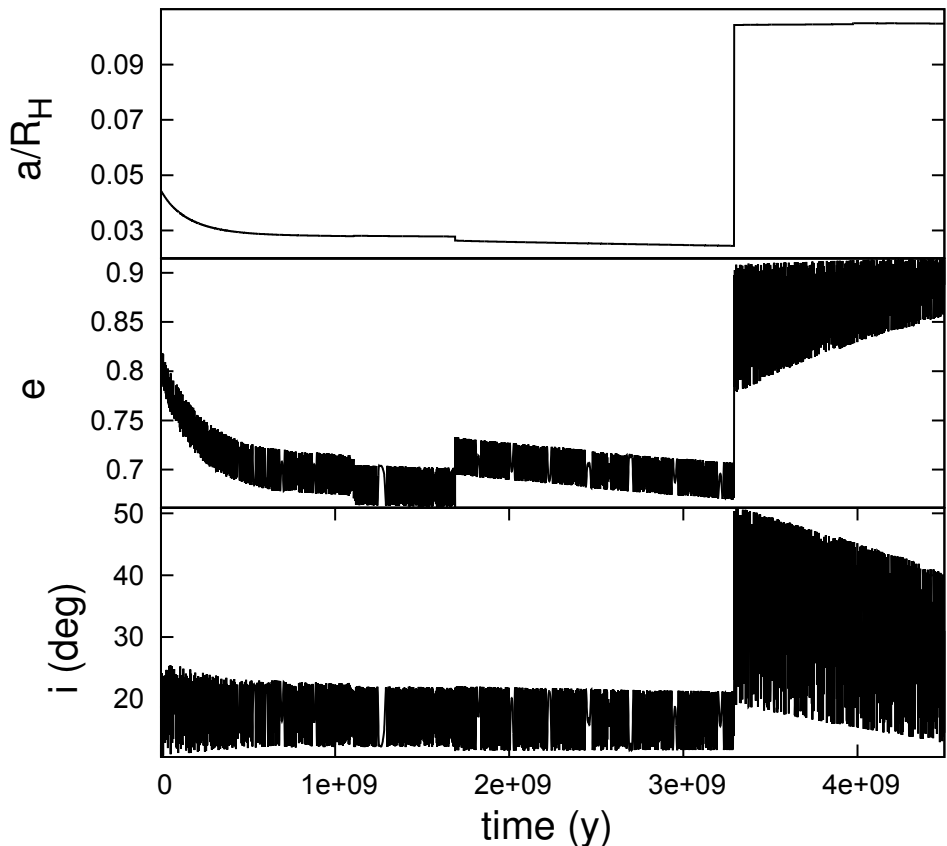


Figure 10: *Cumulative distribution of orbital inclination of ultra wide binaries.*

The distribution of the orbital inclinations is a quantity that may serve as indicative of the formation process of TNBs (Parker & Kavelaars 2012). The cumulative distribution of inclinations of the observed sample of ultra wide binaries (taken from [www.johnstonsarchive.net](http://www.johnstonsarchive.net)) is shown in Fig. (10). For retrograde orbits,  $180^\circ - i$  rather than  $i$  is represented. Ultra wide binaries present roughly equal number of prograde and retrograde orientations. In their collisional evolution model, Parker & Kavelaars (2012) found that it is unlikely for the ultra-wide binaries to have evolved from initially tighter orbits with an initially uniform inclination distribution, because collisions cannot produce a widened population with as cold an inclination distribution as is observed for the ultra-wide binaries. However, Parker & Kavelaars (2012) did not include KCTF evolution in their model. As it was already shown by Porter & Grundy (2012), orbits starting with inclinations near  $90^\circ$  reach very high levels of eccentricity, because of the Kozai mechanism, and therefore initiate a strong tidal friction interaction. These binaries end up tighter than 1 % of  $R_{Hill}$  or become unbound. The cumulative distribution of inclinations of the 20 initially tight binaries which end up as ultra wide ones is depicted in Fig. (10). The agreement with the distribution of the observed sample is remarkable good. These objects are survivors from the region of intermediate inclinations (Porter & Grundy, 2012). After a long period of KCFT evolution, they received a collision which transform them to ultra wide binaries. In Fig. (11) we show the orbital evolution of one of these cases.

1  
2  
3  
4  
5  
6  
7  
8  
9  
10  
11  
12  
13  
14  
15  
16  
17  
18  
19  
20  
21  
22  
23  
24  
25  
26  
27  
28  
29  
30  
31  
32  
33  
34  
35  
36  
37  
38  
39  
40  
41  
42  
43  
44  
45  
46  
47  
48  
49  
50  
51  
52  
53  
54  
55  
56  
57  
58  
59  
60

Figure 11: *The formation of an ultra wide TNB. After KCTF evolution a collision increases the separation of the system .*





## 4 CONCLUSIONS

In this paper we have presented results of numerical simulations of the evolution of a sample of synthetic TNBs under the influence of the solar perturbations, tidal friction, and collisional evolution. We have shown that these effects, acting together, have strongly sculpted the primordial population of TNBs.

For the population of projectiles, we considered the most recent size distributions (Fraser et al. 2014; and Adams et al. 2014). In all the simulation presented here, the population of impactors does not evolve in time. Thus, our results reflect the current collisional environment of the Kuiper Belt.

Numerical simulations that only include KCFT evolution have shown that  $\sim 90\%$  of the primordial TNBs are capable to survive up to the present (Porter & Grundy, 2012). However, if the population of classical TNOs have a power law size distribution as the ones that are inferred from the most recent deep ecliptic surveys (Adams et al. 2014, Fraser et al. 2014), the fraction of surviving binaries at present would be of only  $\sim 70\%$  of the primordial TNB population. The orbits of the surviving systems match reasonably well the observed sample.

Only  $\sim 10\%$  of the objects reach total circularization ( $e \leq 10^{-4}$ , because of the impulse imparted during the collisional process. For the same reason, very few contact binaries should exist in the Trans Neptunian space. Nevertheless, this is not in contradiction with the existence of contact binary comets, such as 8P/Tuttle 67P/Churyumov-Gerasimenko and 103P/Hartley 2, because this end state may be the result of the dynamical evolution as Centaur binaries (Brunini, 2014).

Ultra Wide Binaries are naturally obtained as a result of the combination of the action of KCTF and collisional evolution of an initial population of tight binaries. The population of ultra wide binaries obtained in this way are of 4 – 5 % of the total population of binaries, nearly the observed fraction. In addition, as KCFT evolution prevents the existence of binaries with very high orbital inclinations, the population of ultra wide binaries obtained in this way presents a cumulative distribution of orbital inclinations very similar to the observed distribution. KCTF, and the collisional process, preserve the prograde / retrograde ratio of the initial distribution of orbital inclinations.

Our model does not include a number of effects, such as quadrupole component interaction, that could affect the tidal evolution and the transfer of angular impulse at impacts, and our conclusions should be taken as preliminary. This effect should be included in future models of the dynamical evolution of TNBs.

## References

- Adams, E. R. et al. 2014, AJ, 148, id 55.  
Benz, W. & Asphaug, E. 1999, Icarus, 142, 5-20.  
Brunini, A. 2014, MNRAS, 437, 2297-2302.  
Danby J. M. A., 1988, fcm..book.  
Farinella P., et al. 2000, prpl.conf, 1255.  
Fraser, W. C., et al. 2014, ApJ, 782, id 100.  
Fraser, W. C. & Kavelaars, J. J. 2009, AJ, 137, 72-82.  
Gault, D. E. & Schultz, P. H. 1986, Meteoritics, 21, 368.  
Nesvorný, D., et al. 2011, AJ, 141, id 159.  
Parker, A. H. & Kavelaars, J. J. 2012, ApJ, 744, id. 139.  
Parker, A. H. & Kavelaars, J. J. 2010, ApJ Letters, 722, L204-L208.  
Petit, J.M. & Mousis, O. 2004, Icarus, 168, 409-419.  
Porter, S. & Grundy, W. 2012, Icarus, 220, 947-957.  
Stephen, D. C. & Noll, K. S. 2006, AJ, 131, 1142-1148.  
Yanagisawa, M. & Itoi, T. 1994, Astronomical Society of the Pacific Conference Series, 63, 243.  
Yanagisawa, M. & Hasegawa, S. 2000, Icarus, 146, 270-288.